Iridescence in the neck feathers of domestic pigeons

Haiwei Yin, Lei Shi, Jing Sha, Yizhou Li, Youhua Qin, Biqin Dong, Serge Meyer, Xiaohan Liu,* and Li Zhao
Surface Physics Laboratory and Department of Physics, Fudan University, Shanghai 200433, People's Republic of China

Jian Zi†
Surface Physics Laboratory and Department of Physics, Fudan University, Shanghai 200433, People's Republic of China and T-Center for Life Sciences, Fudan University, Shanghai 200433, People's Republic of China
(Received 24 May 2006; published 22 November 2006)

We conducted structural characterizations, reflection measurements, and theoretical simulations on the iridescent green and purple neck feathers of domestic pigeons (*Columba livia domestica*). We found that both green and purple barbules are composed of an outer keratin cortex layer surrounding a medullary layer. The thickness of the keratin cortex layer shows a distinct difference between green and purple barbules. Green barbules vary colors from green to purple with the observing angle changed from normal to oblique, while purple barbules from purple to green in an opposite way. Both the experimental and theoretical results suggest that structural colors in green and purple neck feathers should originate from the interference in the top keratin cortex layer, while the structure beyond acts as a poor mirror.

DOI: 10.1103/PhysRevE.74.051916 PACS number(s): 42.66.−p, 42.25.−p, 87.19.−j

I. INTRODUCTION

In addition to pigment coloration, structural coloration is another important way of color productions in nature. Structural colors result from the interactions of natural light with microstructures that have a featured size comparable to visible wavelengths via optical phenomena such as interference, diffraction, scattering, or their combinations [1–7]. Structural coloration is rather widespread in the biological world, e.g., in insects [8–16], birds [17–31], and even in plants [32,33].

Structural colors are rather common in avian plumages. The adoption of structural colors in avian plumages may be functional in courtship, camouflage, individuality, or in color signaling and communication as well. Domestic pigeons (*Columba livia domestica*) are descendants of rock doves and can be found almost everywhere throughout the world. Domestic pigeons are rather variable, but usually they have a grey head and body and a dark double wing bar. At the first glance their plumage appears white and grey. However, iridescent green and purple feathers can be found in the neck region of many domestic pigeons. Although some pivotal visible and ultraviolet (UV) reflectance measurements have been already performed with pigeon feathers [18,23,26,34–37], there still have been few detailed reports on the structural origin of the green and purple colors in the iridescent feathers.

In this paper, we study the structural and optical properties of iridescent green and purple neck feathers of domestic pigeons by optical microscope, scanning electron microscopy (SEM), reflectance measurements, and numerical simulations. Our aim is to uncover the structural origin of the iridescent colors in the neck feathers of domestic pigeons and to investigate the correlations between barbule structures and resulting structural colors.

II. STRUCTURAL CHARACTERIZATIONS

Iridescent green and purple neck feathers were plucked off from domestic pigeons bought in a free market in Shanghai. Structural characterizations were done by optical microscope and SEM. The optical microscope images of the iridescent green and purple feathers are shown in Fig. 1. It can be found that each iridescent neck feather consists of a central rachis with an array of barbs projecting on both sides. On each side of a barb there is an array of barbules. Each barbule is composed of successively connected segments. Obviously, the perceived green and purple colors in the iridescent neck feathers arise from barbules. Barbs do not possess any iridescent color.

The cross section of iridescent barbules was characterized by SEM, shown in Fig. 2. All iridescent barbules examined are composed of a central medullary layer surrounded by an outer keratin cortex layer. Barbule thickness is about 2–4 μm. The thickness of the medullary layer varies from 1 to 3 μm. The medulla is composed mainly of randomly dispersed melanin granules in shapes of spheres, ellipses, and rods. There is also a small amount of randomly dispersed keratin. It can be seen that the outer surface of the keratin cortex layer is rather smooth with respect to visible wavelengths.

For barbules with similar color the thickness of the keratin cortex layer is not the same. Instead, it varies in a range

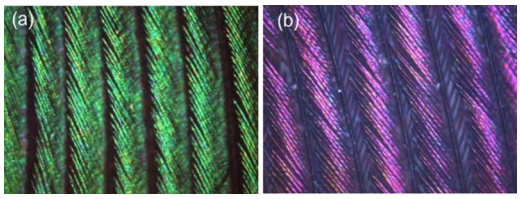

FIG. 1. (Color online) Optical microscope images of iridescent (a) green and (b) purple neck feathers in domestic pigeons under 100× magnification.

*Electronic address: xhiu@fudan.edu.cn
†Electronic address: jzi@fudan.edu.cn

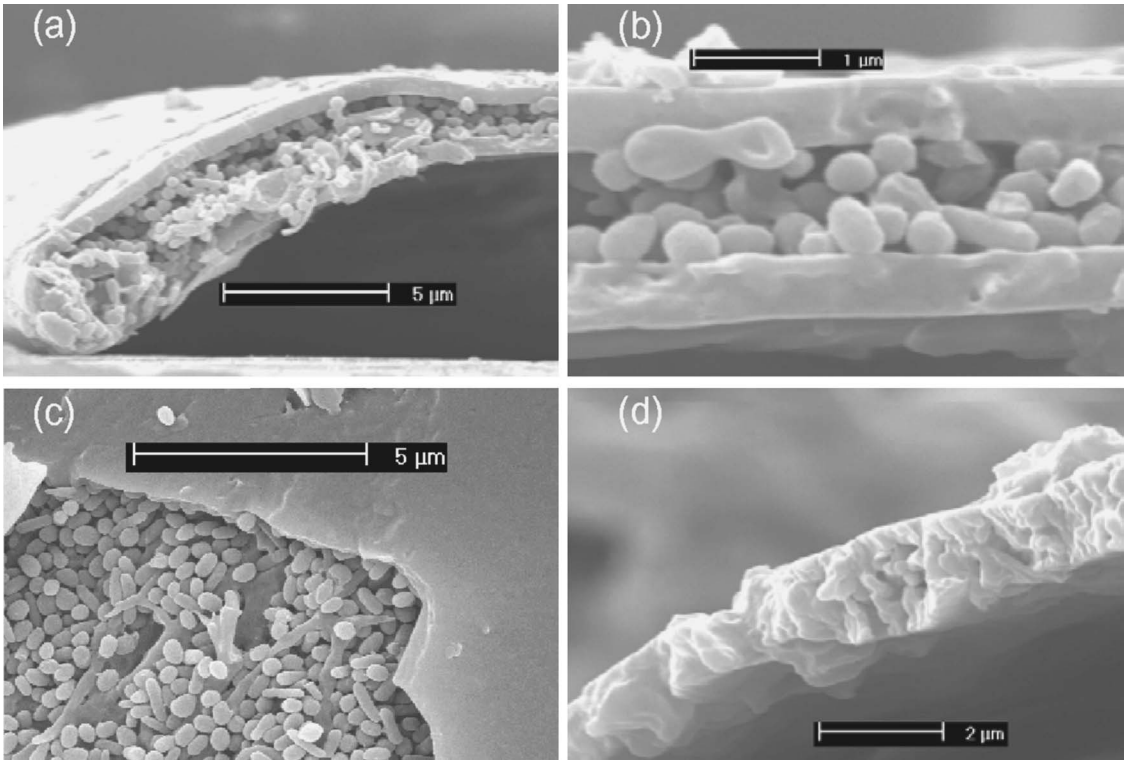

FIG. 2. SEM images of barbules. (a) Perspective view of the cross section of a green barbule. (b) Transverse cross section of a purple barbule. (c) Perspective top view of a green barbule with the top keratin cortex layer removed (lower left corner). (d) Perspective view of the cross section of a grey barbule. Scale bars, (a) 5 μm; (b) 1 μm; (c) 5 μm; (d) 2 μm.

of a few tens of nanometers. Even in a single barbule there are also some thickness fluctuations in the keratin cortex layer. This thickness variation can cause a bit color change. The thickness of the keratin cortex layer for green and purple barbules shows distinct difference. For green barbules under study, the mean thickness is about 595 nm, while that for purple barbules is about 530 nm.

We also characterized the structure of grey barbules. For grey barbules, their structure is distinctly different from that of iridescent barbules. Grey barbules consist of a single uneven layer made from randomly dispersed keratin and melanin granules.

III. REFLECTANCE MEASUREMENTS

The reflection spectra of iridescent green and purple feathers were measured by an optical spectrometer, shown in Fig. 3. Measurements were performed for both normal and oblique incidence. The measured reflection is normalized in order to get a fair comparison. At normal incidence, the iridescent green feather under study exhibits a series of reflection peaks in the measured wavelength range, at about 415, 530, and 730 nm, corresponding to violet, green, and red colors, respectively. With increasing incident angle, all reflection peaks show a blueshift in wavelength. The violet reflection peak at normal incidence shifts to UV wavelength, the green reflection peak to blue wavelength, and the red reflection peak to orange wavelength.

To compare the predicted colors with our perception, a converting method [13] was used to convert a reflectance spectrum into RGB values for a given illuminant. In this paper, we use the CIE (Commission Internationale de l'Éclairage) normalized illuminant D65, which closely matches that of the sky daylight [13]. It is clear that at normal incidence the converted RGB color from the reflection spectrum is green, consistent our perception. This is due to the fact that the reflection peak at 530 nm is dominant in color vision to the human perception. Color changes with incident angles are obvious. At large incident angles, the converted RGB color becomes purple.

At normal incidence the iridescent purple feather under study shows two reflection peaks in the measured wavelength range, at about 465 and 650 nm, corresponding to blue and red color, respectively. The dual reflection peaks lead to a purple color to human perception. The reflection peaks shift to shorter wavelengths with increasing incident angle. At large incident angles, the red reflection peak at normal incidence becomes green in color, while the blue reflection peak at normal incidence shift to violet. As a result, the color of iridescent purple feathers turns into green to human perception at large incident angles. Interestingly, the iridescence change in green and purple feathers is just *opposite*: green feathers become purple and purple feathers change to green in color at large viewing angles.

IV. ORIGIN OF STRUCTURAL COLORS

To explore the origin of structural colors in iridescent feathers, we measured the absolute reflection of a single bar-

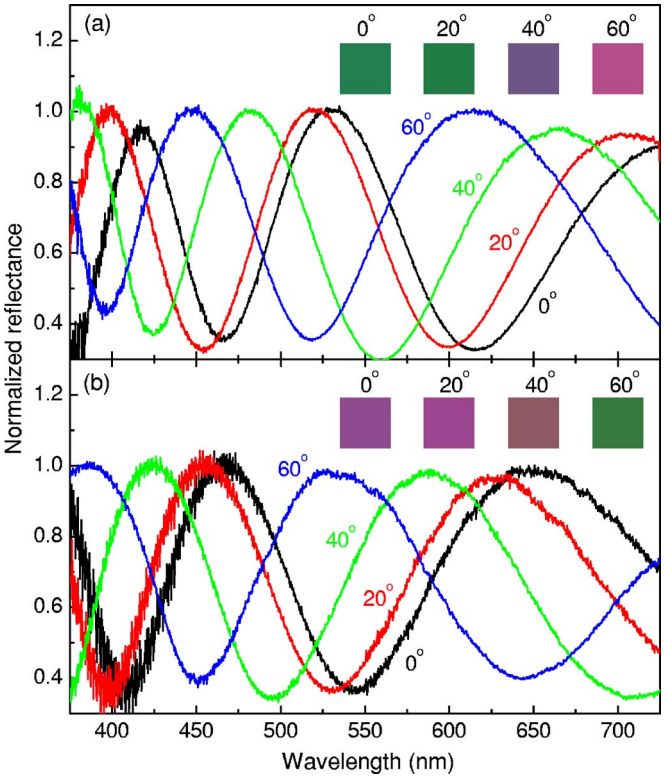

FIG. 3. (Color online) Measured reflection spectra of (a) a green and (b) a purple feather at different incident angles. The converted RGB colors from the reflection spectra at different incident angles are shown in insets.

bule by a reflective microspectroscopy, shown in Fig. 4. In our reflection measurements, we used Al mirrors as the reference. The magnification is 1000× and the objective aperture is 0.9. A field diaphragm was used in order to make the light spot smaller than 2 microns. As a result, the field diaphragm can minimize the incident angle so that it can be considered as normal incidence. Basically, the reflection spectra of green and purple barbules are, respectively, similar to those of green and purples feathers. The reflection peaks measured for barbules coincide with those for feathers although there are some small deviations. This can be expected since there are some thickness fluctuations in the keratin cortex layer. For both green and purple barbules the measured peak reflection is about 20%.

To access the coloration contribution from the medullary layer, we also measured the reflection of a barbule with the top keratin cortex layer removed. In the displayed wavelength range, the measured reflectance is rather low, only about 5%. Thus, most of incident light is absorbed by melanin particles in the medullary layer. The measured reflection spectra for purple barbules show similar features. It can be seen that the measured reflectance of a barbule with the top keratin cortex layer removed shows unspecified features, implying that the medullary layer gives nearly no contribution to structural coloration. We can thus conclude that the structural coloration in green and purple barbules result predominantly from the top keratin cortex layer alone.

From the interference theory we know that for a thin film with a fixed refractive index there appears a series of harmonic reflection peaks with equal intensity. Moreover, the frequency interval between adjacent harmonic reflection peaks is identical. From the measured reflection spectra of iridescent feathers or barbules, we can notice that the intensities of reflection peaks are rather similar and the frequency interval between reflection peaks is nearly identical for both normal and oblique incidence. These facts suggest that structural colors in iridescent barbules should originate from the thin-film interference of the top keratin cortex layer alone. Although the medullary layer does not contribute to structural coloration, it does give some contributions to the brightness.

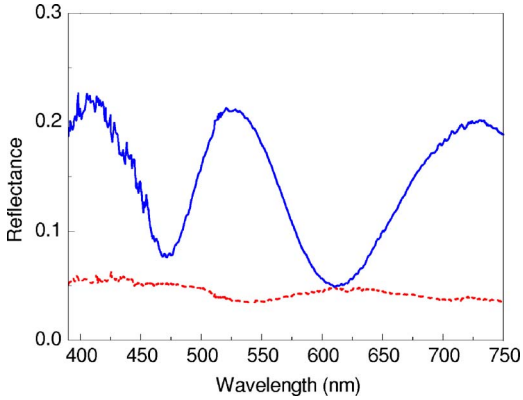

FIG. 4. (Color online) Measured reflection spectrum (solid line) of a green barbules at normal incidence. The dashed line denotes the measured reflection spectrum for a green barbule with the top keratin cortex layer removed [see Fig. 2(c)].

V. THEORETICAL MODELING

Based on the structural characterizations and reflection measurements, we revealed that the structural colors in iridescent barbules come from the thin-film interference of the top keratin cortex layer. The low and featureless reflectance of a barbule with the top keratin cortex layer removed indicates that the structural part below the top keratin cortex layer does not contribute to structural coloration. Instead, it plays a role of a poor mirror. Reflected light by this poor mirror does not contribute to interference and its reflection should show a weak wavelength dependence since the medulla consists of randomly dispersed melanin particles. Therefore, the observed reflection R results from the interference in the top keratin cortex layer and the reflection from the poor mirror, namely,

$$R = R_1 + (1 - R_1)R_2(1 - R_1), \tag{1}$$

where R_1 is the reflectance of the top keratin cortex alone and R_2 is the reflection of the poor mirror. From Fig. 4, we can determine $R_2 \simeq 5\%$ in the measured wavelength range. For a thin-film in air ambiance, its reflectance is given by [38]

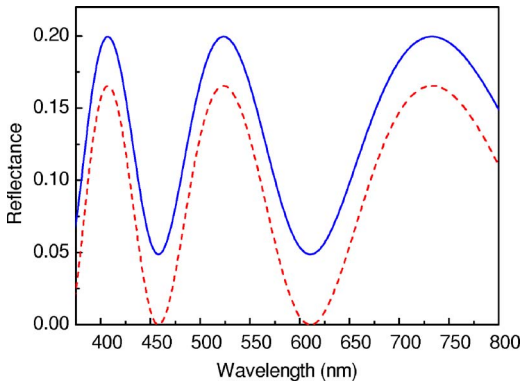

FIG. 5. (Color online) Predicted reflectance (solid line) at normal incidence for a 595 nm keratin thin film with (solid line) and without (dashed line) a poor mirror introduced.

$$R_1 = \frac{4r^2\sin^2(2\pi d\sqrt{n^2-\sin^2\theta}/\lambda)}{(1-r^2)^2+4r^2\sin^2(2\pi d\sqrt{n^2-\sin^2\theta}/\lambda)}, \tag{2}$$

where λ is the vacuum wavelength, θ is the incident angle, d and n are, respectively, the thickness and refractive index of the thin film. There are two independent polarizations, one with the electric field perpendicular to the plane formed by the surface normal and incident ray (s polarization) and another one with the magnetic field perpendicular to the plane (p polarization). The reflection coefficient r at the air/keratin interface is different for different polarizations, given by

$$r_s = \frac{\cos\theta - \sqrt{n^2-\sin^2\theta}}{\cos\theta + \sqrt{n^2-\sin^2\theta}}, \tag{3a}$$

$$r_p = \frac{n^2\cos\theta - \sqrt{n^2-\sin^2\theta}}{n^2\cos\theta + \sqrt{n^2-\sin^2\theta}}. \tag{3b}$$

It can be seen from Eq. (2) that there exists a series of harmonic reflection peaks. Moreover, the frequency difference between two adjacent harmonic reflection peaks is equal. It can be shown that the wavelengths of the harmonic reflection peaks for both s and p polarizations are given by

$$\lambda_m = \frac{2d\sqrt{n^2-\sin^2\theta}}{m+1/2}, \tag{4}$$

where m is the order index of the harmonic peaks and takes the values of $0,1,2,\ldots$. For unpolarized incident light the reflectance of the thin film is the superposition of the contributions from s and p polarizations, namely, $R_1=(R_{1s}+R_{1p})/2$, where R_{1s} and R_{1p} are the reflections for s and p polarization, respectively.

Figure 5 shows the predicted reflection of a keratin thin-film with a thickness of 595 nm situated on a poor mirror with a reflection of 5%. The refractive index of keratin is assumed to be $n=1.54$, taken from [21]. It is obvious that the predicted reflection agrees well with the measured one shown in Fig. 4. If the poor mirror is not introduced, the predicted peak reflectance is smaller than experimental results. Moreover, the minimum reflectance is zero. These facts confirm the validity of treating the structure below the top keratin layer as a poor mirror. From Eq. (4) we can determine the order index of the observed reflection peaks. For green barbules the observed reflection peaks at red, green, and violet wavelength correspond to the second, third, and fourth order harmonic reflection peaks, respectively. The observed red and blue reflection peaks of purple barbules correspond, respectively, to the second and third order harmonic reflection peaks. The fundamental (0th order) and the first order harmonic reflection peaks of both green and purple barbules are in the infrared region. Higher order harmonic reflection peaks are in the UV region.

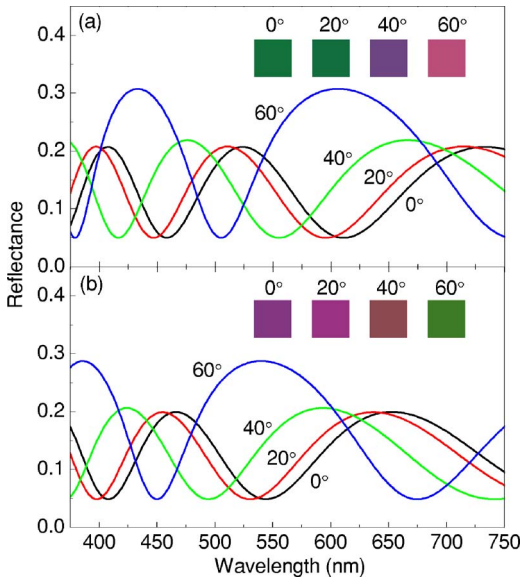

FIG. 6. (Color online) Predicted reflectance for (a) green and (b) purple barbules at different incident angles. The converted RGB colors from the reflection spectra at different incident angles are shown in insets.

Due to the limitation of our optical spectrometer, we cannot measure the reflection spectra in the UV region. McGraw [37] did UV reflection measurements on iridescent green and purple neck feathers of domestic pigeons and found that both green and purple feathers show UV reflection peaks. From our analysis, it can be determined that the observed UV reflection peaks come also from the thin-film interference in the keratin cortex layer.

Under the theory introduced above, we can also calculate the reflection spectra of both green and purple barbules at oblique incident angles in order to investigate their iridescence, shown in Fig. 6. Both green and purple barbules are modeled as a keratin thin film situated on a poor mirror with a reflectance of 5%. The thickness of the keratin thin film for green barbules is 595 nm and that for purple barbules is 530 nm. The wavelengths of all harmonic reflection peaks undergo a blueshift with increasing incident angle. For green barbules, the second order harmonic reflection peak shifts wavelength from red at normal incidence to orange at large incident angles. The third order harmonic reflection peak shifts wavelength from green at normal incidence to blue at oblique incidence. The fourth order harmonic reflection peak changes wavelength from violet to UV with increasing incident angle. We also calculate the RGB colors from the pre-

TABLE I. Calculated *XYZ* color for green and purple barbules at different incident angles.

	Green barbule			Purple barbule		
Incident angle (deg.)	*X*	*Y*	*Z*	*X*	*Y*	*Z*
0	0.088	0.133	0.103	0.128	0.101	0.176
20	0.081	0.121	0.104	0.146	0.110	0.185
40	0.120	0.105	0.171	0.175	0.157	0.156
60	0.253	0.209	0.256	0.185	0.252	0.126

dicted reflection spectra. Obviously, the converted RGB color is green at normal incidence and becomes purple at large incident angles. The converted RGB colors from the predicted reflection spectra agree well with those from the measured ones shown in Fig. 3(a).

For purple barbules the second order harmonic reflection peak shifts wavelength from red at normal incidence to green at oblique incidence. The third order harmonic reflection peak changes wavelength from blue at normal incidence to violet at large incident angles. It is obvious that the converted RGB color shows a color change from purple at normal incidence to green at large incidence angles, consistent with experimental results shown in Fig. 3(b).

The RGB color space cannot always produce a color equivalent to any wavelength. The red component sometimes should be negative or great than one in order to produce these colors. This means that not all visible colors can be produced using the RGB system. Moreover, RGB is an device-dependent color model: the color one gets depends on the device. On the other hand, the *XYZ* colors defined by the CIE in 1931 are device independent. Therefore, from an ethological point of view, it is of interest to give the *XYZ* colors of pigeon green and purple barbules, shown in Table I.

VI. DISCUSSIONS

It is rather interesting that structural colors in domestic pigeon neck feathers take advantage of a single keratin thin film rather than a multilayer reflector which is rather common in the biological world [4]. It is known that the reflection from a multilayer reflector is very high, leading to a high brightness for structural coloration. On the contrary, the brightness resulting from a single thin film is rather low. This can be understood by the fact that in the single thin film there are only two interfaces involved in constructive interference, while there is multiple interference in the multilayer reflector. The adoption of a single thin film to produce structural coloration in the iridescent neck feathers may be biologically significative: the low brightness of structural colors is highly advantageous to avoid predators, while vision information can still be conveyed.

It is rather interesting to note an early work of reflection measurements on pigeon neck feathers done in 1925 [18]. Based on the measured reflection spectra at difference incident angles, it was inferred that the structural color and iridescence in pigeon neck feathers might originate from interference of a thin film with a thickness of 208 nm and the reflection peak in the visible range was due to the first order harmonic reflection peak. Our structural measurements indicate that the thickness of the thin film that gives rise to structural colors are much larger than that conjectured in Ref. [18]. Moreover, both our experimental and theoretical results suggest that the second and higher order harmonic reflection peaks are responsible for structural colors instead of the first order one.

Iridescence is one of the distinct properties of structural coloration. For viewing angles changed from normal to oblique green feathers vary color form green to purple. On the contrary, purple feathers change color from purple to green in an opposite way. Consequently, both green and purple colors can be perceived no matter what the observing angle is or how green and purple feathers are arranged. This opposite iridescence may render maximal information signaling and communication possible. For two multilayer reflectors, it is difficult to cause such opposite iridescence. By contrast, it is easy to obtain opposite iridescence by the single thin-film interference due to the fact that the harmonic reflection peaks can be altered simply by changing the thin-film thickness. We can thus conclude that the adoption of the single thin-film interference to produce structural colors in the iridescent neck feathers of domestic pigeons is not accidental. Instead, it should be a result of careful designs by nature.

VII. CONCLUSION

We studied the structural properties of iridescent green and purple neck feathers in domestic pigeons by using optical microscope and SEM. Both green and purple barbules are found to be composed of a medullary layer surrounded by an outer keratin cortex layer. Grey barbules, however, do not possess such a structure so that they do not possess any structural color. Reflection measurements reveal that there is interesting opposite iridescence in green and purple barbules: with varying viewing angle from normal to oblique, green barbules change color from green to purple, while purple barbules from purple to green in an opposite way. Both experimental and theoretical results indicate that structural colors in both green and purple barbules result from the interference in the top keratin cortex layer alone. The structure beyond the top keratin cortex layer plays a role of a poor mirror in order to enhance a bit the brightness. The observed opposite iridescence in green and purple feathers may contain important biological implications in color signaling and communication.

ACKNOWLEDGMENTS

This work was mostly supported by the CNKSRSF Grant No. 2006CB0L0906. Partial support from NSFC, PCSIRT, and Shanghai Science and Technology Commission is also acknowledged. One of the authors (JZ) is grateful to Professor R. O. Prum for stimulating discussions and suggestions.

[1] M. F. Land, Prog. Biophys. Mol. Biol. **24**, 75 (1972).
[2] D. L. Fox, *Animal Biochromes and Structural Colors* (University of California Press, Berkeley, CA, 1976).
[3] M. Srinivasarao, Chem. Rev. (Washington, D.C.) **99**, 1935 (1999).
[4] A. R. Parker, J. Opt. A, Pure Appl. Opt. **2**, R15 (2000).
[5] P. Vukusic and J. R. Sambles, Nature (London) **424**, 852 (2003).
[6] S. Kinoshita and S. Yoshioka, ChemPhysChem **6**, 1442 (2005).
[7] A. R. Parker, J. R. Soc., Interface **2**, 1 (2005).
[8] A. Mallock, Proc. R. Soc. London, Ser. A **85**, 598 (1911).
[9] C. W. Mason, J. Phys. Chem. **31**, 321 (1927); **31**, 1856 (1927).
[10] T. D. Schultz and G. D. Bernard, Nature (London) **337**, 72 (1989).
[11] A. R. Parker, D. R. Mckenzie, and M. C. J. Large, J. Exp. Biol. **201**, 1307 (1998).
[12] P. Vukusic, J. R. Sambles, C. R. Lawrence, and R. J. Wootton, Proc. R. Soc. London, Ser. B **266**, 1402 (1999).
[13] B. Gralak, G. Tayeb, and S. Enoch, Opt. Express **9**, 567 (2001).
[14] P. Vukusic, J. R. Sambles, C. R. Lawrence, and R. J. Wootton, Proc. R. Soc. London, Ser. B **269**, 7 (2002).
[15] A. R. Parker, V. L. Welch, D. Driver, and N. Martini, Nature (London) **426**, 786 (2003).
[16] J. P. Vigneron, J.-F. Colomer, N. Vigneron, and V. Lousse, Phys. Rev. E **72**, 061904 (2005).
[17] C. W. Mason, J. Phys. Chem. **27**, 201 (1923).
[18] E. Merritt, J. Opt. Soc. Am. **11**, 93 (1925).
[19] C. H. Greenwalt, W. Brandt, and D. D. Friel, J. Opt. Soc. Am. **50**, 1005 (1960).
[20] J. Dyck, Biol. Skr. (Copenhagen) **18**, 1 (1971).
[21] J. Dyck, Z. Zellforsch Mikrosk Anat. **115**, 17 (1971).
[22] H. Durrer, In *Biology of the Integument. 2. Vertebrates*, edited by J. Bereiter-Hahn, A. G. Matoltsky, and K. S. Richards (Springer, Berlin, 1986), p. 239.
[23] J. Dyck, Biol. Skr. (Copenhagen) **30**, 2 (1987).
[24] R. O. Prum, R. Torres, S. Williamson, and J. Dyck, Nature (London) **396**, 28 (1998).
[25] R. O. Prum, R. H. Torres, S. Williamson, and J. Dyck, Proc. R. Soc. London, Ser. B **266**, 13 (1999).
[26] D. Osorio and A. D. Ham, J. Exp. Biol. **205**, 2017 (2002).
[27] M. D. Shawkey, A. M. Estes, L. M. Siefferman, and G. E. Hill, Proc. R. Soc. London, Ser. B **270**, 1455 (2003).
[28] J. Zi, X. D. Yu, L. Z. Li, X. H. Hu, C. Xu, X. J. Wang, X. H. Liu, and R. T. Fu, Proc. Natl. Acad. Sci. U.S.A. **100**, 12576 (2003).
[29] D. J. Brink and N. G. van der Berg, J. Phys. D **37**, 813 (2004).
[30] Y. Li, Z. Lu, H. Yin, X. Yu, X. Liu, and J. Zi, Phys. Rev. E **72**, 010902(R) (2005).
[31] J. P. Vigneron, J.-F. Colomer, M. Rassart, A. L. Ingram, and V. Lousse, Phys. Rev. E **73**, 021914 (2006).
[32] D. W. Lee, Am. Sci. **85**, 56 (1997).
[33] J. P. Vigneron, M. Rassart, Z. Vértesy, K. Kertész, M. Sarrazin, L. P. Biró, D. Ertz, and V. Lousse, Phys. Rev. E **71**, 011906 (2005).
[34] D. S. Blough, J. Opt. Soc. Am. **47**, 827 (1957).
[35] A. A. Wright, J. Iowa Med. Soc. **17**, 325 (1972).
[36] J. K. Bowmaker, Vision Res. **17**, 1129 (1977).
[37] K. J. McGraw, Naturwiss. **91**, 125 (2004).
[38] M. Born and E. Wolf, *Principles of Optics* (Cambridge University Press, Cambridge, 1999).